

Symbolic Control for Autonomous Docking of Marine Surface Vessels

Elizabeth Dietrich*, Emir Cem Gezer*, Bingzhuo Zhong, *Member, IEEE*,
Murat Arca, *Fellow, IEEE*, Majid Zamani, *Senior Member, IEEE*,
Roger Skjetne, *Senior Member, IEEE*, and Asgeir Johan Sørensen, *Senior Member, IEEE*

Abstract—Docking marine surface vessels remains a largely manual task due to its safety-critical nature. In this paper, we develop a hierarchical symbolic control architecture for autonomous docking maneuvers of a dynamic positioning vessel, to provide formal safety guarantees. At the upper-level, we treat the vessel’s desired surge, sway, and yaw velocities as control inputs and synthesize a symbolic controller in real-time. The desired velocities are then transmitted to and executed by the vessel’s low-level velocity feedback control loop. Given a synthesized symbolic controller, we investigate methods to optimize the performance of the proposed control scheme for the docking task. The efficacy of this methodology is evaluated on a low-fidelity simulation model of a marine surface vessel in the presence of static and dynamic obstacles and, for the first time, through physical experiments on a scaled model vessel.

Index Terms—Marine Robotics, Hybrid Logical/Dynamical Planning and Verification, Robot Safety, Correct-by-construction Synthesis, Symbolic Controllers

I. INTRODUCTION

In recent decades, there has been an increasing demand for enhancing the efficiency and operational safety of marine surface vessels (MSV) through the development of autonomy [1]. While low-level automatic control functionalities, such as dynamic positioning [2] are well studied, significant challenges remain in high-level control tasks like automatic path planning, collision avoidance, and guidance, as they are typically complex logical tasks and the corresponding controller synthesis over continuous (hybrid) systems is challenging. Traditionally, these tasks have been performed by operators who rely heavily on training, experience, situational awareness, and risk understanding. In contrast, autonomy leverages advanced sensing, computation, and control capabilities, offering the

*Both authors contributed equally to this research.

E. Dietrich and M. Arca are with the Department of Electrical Engineering and Computer Sciences, University of California, Berkeley, USA. Email: {eadietri, arcak}@berkeley.edu

E. C. Gezer, R. Skjetne and A. J. Sørensen are with the Centre for Autonomous Marine Operations and Systems, Department of Marine Technology, Norwegian University of Science and Technology, Trondheim, Norway. Email: {emir.cem.gezer, roger.skjetne, asgeir.sorensen}@ntnu.no

B. Zhong is with the Thrust of Artificial Intelligence, Information Hub, Hong Kong University of Science and Technology (Guangzhou), China. Email: bingzhuoz@hkust-gz.edu.cn

M. Zamani is with the Department of Computer Science, University of Colorado Boulder, USA. Email: majid.zamani@colorado.edu

This work has been submitted to the IEEE for possible publication. Copyright may be transferred without notice, after which this version may no longer be accessible.

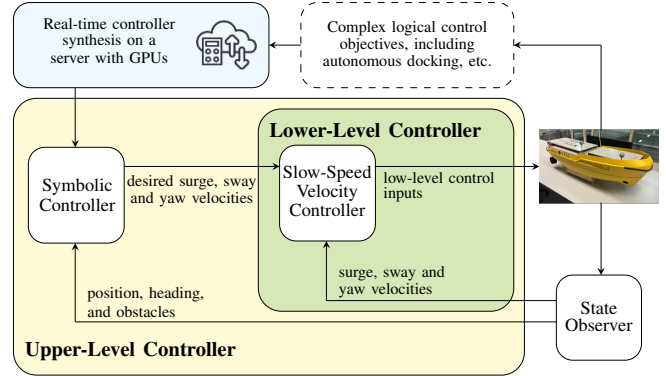


Fig. 1. Symbolic control scheme for Dynamic Positioning (DP) vessels with low-level velocity feedback control loop.

potential to enhance safety, improve usage of human resources, reduce environmental impact, and minimize human injuries and fatalities at sea.

Docking is among the various complex high-level control tasks for an MSV. When a vessel approaches a harbor for docking, it first enters the harbor basin where it must safely maneuver to a docking location while avoiding structures and other vessels; this is often referred to as the approach phase. After approaching the target docking location, the vessel’s auto-docking system will ensure the vessel is brought slowly and safely to berth. Docking is a highly complex maneuver that largely remains manually performed due to the high risk of collision and strict precision requirements [3]. In this paper, we focus on the approach phase of the docking operation. Specifically, we aim to design a *correct-by-construction* control scheme for safe autonomous docking using rigorous tools from control theory and formal methods [4]. These tools, originating in computer science, are intended to ensure the correct operation of computer programs and digital circuits. Further, they offer formal guarantees, allowing us to derive controllers in a provable fashion. The correct-by-construction methodology, an emerging technique for safe autonomy over the past decade, represents a significant improvement over the common practice of verification after design completion [5], which typically necessitates extensive testing and re-design cycles.

In the context of correct-by-construction synthesis, abstraction-based approaches (a.k.a. symbolic control) have been explored for various systems, including linear systems [6], nonlinear systems with bounded disturbances [7],

and nonlinear stochastic games [8]. Specifically, a finite abstraction (*symbolic system*) with finite states and input sets is first constructed as a simplified version of the original continuous system. Controllers are then synthesized over the symbolic system to meet complex logical high-level control objectives and subsequently refined back to the original system to achieve formal safety guarantees. However, because the finite state and input sets are created by partitioning the original sets with grids, applying these approaches to real-world applications is challenging due to their computational complexity.

Contribution: In this paper, we propose a hierarchical symbolic control scheme to address the safe autonomous docking problem for Dynamic Positioning (DP) vessels, potentially extending to more complex logical control objectives, as illustrated in Fig. 1. At the upper-level, leveraging the vessel's kinematic model with desired surge, sway, and yaw velocities as control inputs, a symbolic controller is synthesized in real-time using the approach in [9]. The desired velocities are then transmitted to and executed by a low-speed velocity feedback control loop in the DP control system, at the lower-level. To achieve real-time synthesis of the symbolic controller, we deploy pFaces [10] on a server to enable parallel computation for the synthesis procedure with graphics processing units (GPUs), thus mitigating the computational bottleneck of symbolic control methodologies. Furthermore, given a synthesized symbolic controller, we investigate methods to optimize performance for safe autonomous harbor maneuvering. The effectiveness of the proposed control scheme is validated on a low-fidelity simulation model of a MSV and, for the first time, through physical experiments on a scaled model vessel.

Related Works: Although docking is mostly performed manually due to its safety-critical nature, autonomous docking has gained increasing attention over the past decades [3]. Existing autonomous docking methods typically deploy various path planning algorithms, such as Dubins curves [11], A* [12], and State-lattice [13], combined with accurate navigation systems and electronic nautical charts. The paths are then tracked using different control methodologies, including PID [14], adaptive control [15], model predictive control [16], and artificial neural networks [17]. However, due to the heuristic nature of many of these approaches and the safety-critical aspect of docking, the corresponding control software must be verified to ensure safety levels at least equivalent to those of human-navigated vessels [18]. Additionally, these approaches still have limitations in handling dynamic obstacles and situational awareness [3]. In contrast, the symbolic control scheme we use here provides inherent safety guarantees. These formal guarantees are achieved through the correct-by-construction synthesis paradigm, and the proposed real-time controller synthesis mechanism allows adaptation to dynamic obstacles and environments. While [19] also utilized correct-by-construction synthesis for safe autonomous harbor maneuvering, the controller was synthesized offline, and no physical experiments were conducted to validate the proposed results. Although symbolic control was hampered by computational complexity in the past, real-time synthesis is now becoming possible with parallel computation and GPUs [20], [21]. This

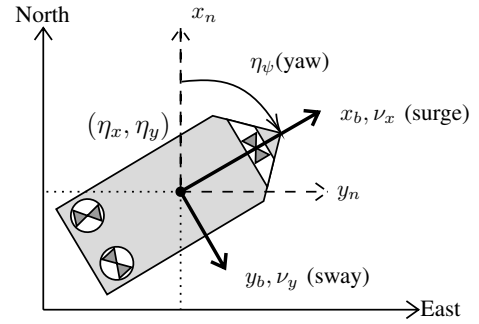


Fig. 2. Coordinate frame of marine vessel control system. The vessel is equipped with two azimuth thrusters and one tunnel thruster. The vessel's position is described by vector η . The subscript n refers to the world-fixed frame, while the subscript b refers to the body-fixed frame.

paper contributes to the ongoing efforts and demonstrates symbolic control on autonomous docking maneuvers with experiments on a scale marine vessel.

Organization: The system dynamics are introduced in Section II. In Section III, a hierarchical symbolic control strategy is utilized to synthesize and implement a control law for safe autonomous docking of a vessel. The experimental setup is introduced in Section IV, followed by the simulation and experimental results in Section V.

II. SYSTEM DYNAMICS

The motion of surface vessels has been extensively studied; see e.g. [22]. In this project, we use a three degrees of freedom (3-DOF) maneuvering ship model that considers only surge, sway, and yaw motion. The vessel's dynamics are modeled in a body-fixed frame with respect to a world-fixed frame, as shown in Fig. 2.

A. Kinematics

The kinematic model describes the relationship between the vessel's body-fixed velocities and its position and orientation in the world-fixed frame. This relationship is expressed as

$$\dot{\eta} = \mathbf{R}(\eta_\psi)\nu, \quad \mathbf{R}(\eta_\psi) = \begin{bmatrix} \cos \eta_\psi & -\sin \eta_\psi & 0 \\ \sin \eta_\psi & \cos \eta_\psi & 0 \\ 0 & 0 & 1 \end{bmatrix}, \quad (1)$$

where $\eta = [\eta_x, \eta_y, \eta_\psi]^T$ represents the vessel's position (η_x, η_y) and orientation (η_ψ) in the world-fixed frame. Furthermore, $\nu = [\nu_x, \nu_y, \nu_\psi]^T$ denotes the vessel's linear and angular velocities in the body-fixed frame, corresponding to surge, sway, and yaw motions, respectively. $\mathbf{R}(\eta_\psi)$ is the rotation matrix that transforms velocities from the body-fixed frame to the world-fixed frame. In this work, linear velocities are expressed in meters per second (m/s) and angular velocities in radians per second (rad/s), unless stated otherwise.

B. Kinetics

The kinetic model describes the forces and moments acting on the vessel and their effect on its velocity. The kinetics of the 3-DOF motion are given by

$$\mathbf{M}\dot{\nu} + \mathbf{C}(\nu)\nu + \mathbf{D}(\nu)\nu = \tau + b, \quad (2)$$

where $\mathbf{M} \in \mathbb{R}^{3 \times 3}$ is the inertia matrix, including the vessel's mass and added mass terms, $\mathbf{C}(\nu) \in \mathbb{R}^{3 \times 3}$ represents Coriolis and centripetal forces, $\mathbf{D}(\nu) \in \mathbb{R}^{3 \times 3}$ is the hydrodynamic damping matrix accounting for drag forces, $\tau \in \mathbb{R}^3$ represents the control forces and moments applied to the vessel (e.g., thrusters), and $b \in \mathbb{R}^3$ represents unmodeled dynamics and slowly varying environmental loads. From (2), the vessel's acceleration in terms of the control input τ is:

$$\dot{\nu} = \mathbf{M}^{-1}(\tau - \mathbf{C}(\nu)\nu - \mathbf{D}(\nu)\nu + b). \quad (3)$$

III. CONTROL STRATEGY

The goal is to design a correct-by-construction hierarchical control architecture for a surface vessel that synthesizes a symbolic controller in real-time to enhance performance in autonomous harbor and docking maneuvers while avoiding obstacles. In Fig. 1, we highlight the upper-level and lower-level controllers of this architecture. We provide an explanation of symbolic control in Section III-A to describe the formation of the upper-level controller, and in Section III-B we elaborate on the low-level velocity control loop.

A. Symbolic Control

Symbolic control [7], [23]–[25] is an approach to derive provably safe controllers that satisfy complex logical specifications including objectives and constraints in linear temporal logic, a tool for reasoning about propositions qualified in terms of time. Symbolic control relies on the existence of a symbolic system which is a simplified, finite abstraction of the continuous system. We utilize the approach presented in [7] to obtain an abstraction of our system through a feedback refinement relation that ensures our symbolic model contains all of the behaviors of the vessel's physical model.

The closed loop resulting from this approach can be seen in Fig. 3. We create a *symbolic controller* that consists of a quantizer and an abstract controller synthesized over the finite abstraction that is usually computed in the form of a finite automaton whose states are a result of the quantized plant model. The symbolic controller outputs a list of possible control actions that satisfy a given specification. We optimize over this list to determine the optimal control input for our system, a vessel. This results in a velocity command that is given back to the vessel and executed by a low-level velocity controller, as shown in Fig. 1.

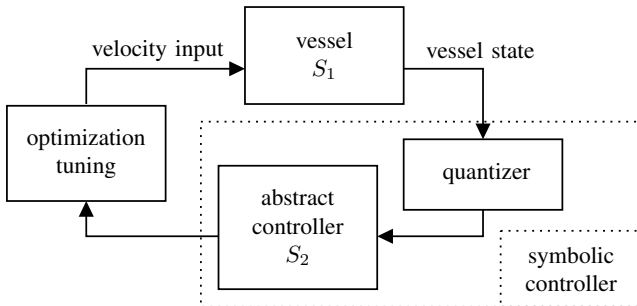


Fig. 3. Closed loop resulting from the abstraction, refinement, and optimization approach, adapted from [7, Fig. 1].

Let us consider the control problem associated with the autonomous harbor and docking maneuvers from our two obstacle real-world experiments. We adopt the convention that the states of system i are denoted with subscript i and $[a, b]$ denotes a discrete interval. We seek to guide the vessel (1) throughout a region with boundary, B , into a target docking position, T_1 , while avoiding obstacles O_1^1 and O_1^2 as seen in Fig. 4. We measure the state of the vessel and provide control inputs every 2 seconds. This formulates our control problem (S_1, Σ_1) where S_1 is a mathematical representation of the physical vessel model and Σ_1 is the following specification

$$\begin{aligned} \{(u, x) \in (U_1 \times X_1)^{\mathbb{Z}^+} | x(0) \in B \setminus (O_1^1, O_1^2) \\ \Rightarrow \forall t \in \mathbb{Z}^+ (x(t) \notin \{O_1^1, O_1^2\} \wedge \exists t' \in [t, \infty) x(t') \in T_1)\}, \end{aligned} \quad (4)$$

with $U_1 = [-0.2, 0.2] \times [-0.2, 0.2] \times [-0.3, 0.3]$ as the set of inputs, and $X_1 = \mathbb{R}^2 \times [-\pi, \pi]$ as the set of vessel states.

To synthesize an abstract controller, we need to form a finite-state approximation of S_1 . The resulting abstraction, S_2 , is built using a feedback refinement relation. Intuitively, every state of S_2 will be associated to a subset of the state set of S_1 based on the refinement relation, and S_2 will have imposing relations among its states to represent the dynamics of the original system. These relations are defined as a transition function, as discussed below. In a general sense, S_2 will fully contain the behavior of S_1 ; however, S_2 is a finite-state approximation of our control problem over which the control synthesis problem can be solved using standard search algorithms.

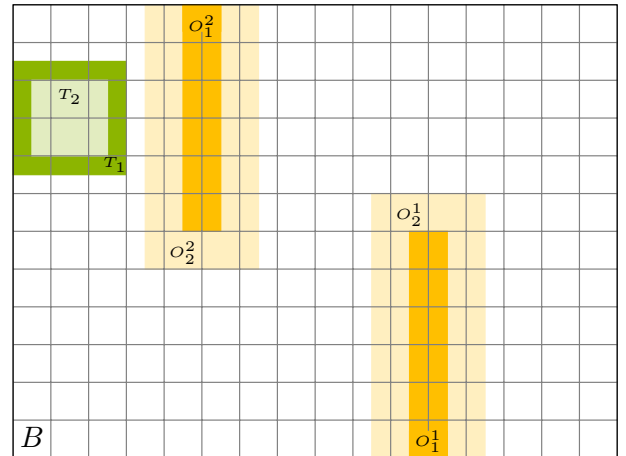


Fig. 4. Discretized system with boundary $B = 8m \times 6m$ and states of S_1 and S_2 . S_1 has obstacles O_1^1 and O_1^2 (dark orange) and target docking position, T_1 (dark green). S_2 has obstacles O_2^1 and O_2^2 (light orange) and target docking position, T_2 (light green).

S_2 is connected to the plant via a static quantizer, irrespective of the specification imposed on the plant. Additionally, in defining S_2 , we introduce margins for over-approximations of obstacles and an under-approximation for the target docking position. This can be seen in Fig. 4 as O_2^1 , O_2^2 , and T_2 . These margins account for the geometrical shape of the vessel. Alternatively, they can be set according to other factors, e.g. [26], [27]. Therefore, the abstract specification, Σ_2 , of our

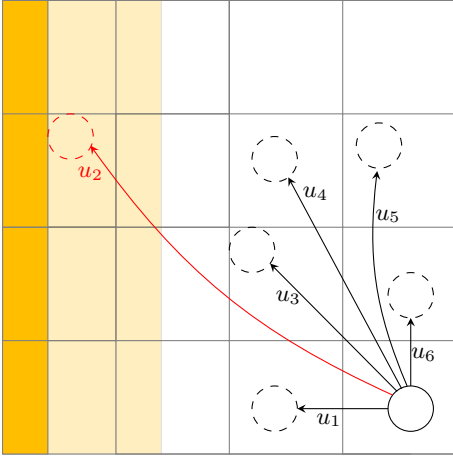


Fig. 5. Possible transitions from vessel state (solid circle) to locations in the state space (dashed circles). The controller synthesis procedure will eliminate u_2 as a viable control action since it results in an unsafe maneuver (the vessel would collide with the orange obstacle). The list of possible control inputs returned would consist of u_1, u_3, u_4, u_5 , and u_6 .

system is (4) where we substitute O_1^1, O_1^2, T_1 with O_2^1, O_2^2, T_2 , respectively.

The abstract system, S_2 , has an associated transition function that defines the relationship amongst its states. This transition function represents the plant behavior and determines where in the state space the plant may transition. Fig. 5 illustrates a transition function. A standard search algorithm [24] is performed to determine safe control commands that allow the vessel to achieve its goal position. A list of all possible control actions that solve this problem are returned each time the synthesis task is performed with an updated vessel position.

Once a list of safe possible actions is computed, the plant may be given any one of the control commands. Every action on this list will result in safe progress towards the plant's goal. We present an approach to optimize this selection process for realistic vessel behavior. The optimal control action is chosen using a cost function that favors forward motion and reduces the norm between sequential control actions. Let $\mathcal{A} = \{\sigma_1, \sigma_2, \dots, \sigma_n\}$ be a list of actions where $\sigma_i \in \mathbb{R}^3$, σ_{pre} be the previously chosen action, and $\Delta\sigma_i := \sigma_i - \sigma_{pre}$. We define the cost function $J(\sigma_i)$ as

$$J(\sigma_i) = \beta(\sigma_i)^T W_i \beta(\sigma_i), \quad \beta(\sigma_i) = \begin{bmatrix} \sigma_i \\ \Delta\sigma_i \end{bmatrix} \in \mathbb{R}^6, \quad (5)$$

where $W \in \mathbb{R}^{6 \times 6}$ is positive semi-definite. We select the control action that minimizes the cost

$$\nu_{ref} := \sigma^* = \arg \min_{\sigma_i \in \mathcal{A}} J(\sigma_i). \quad (6)$$

B. Velocity Feedback Controller

The velocity feedback controller, illustrated in Fig. 6, controls the vessel's surge, sway, and yaw velocities, represented by ν_{ref} , using a Multiple-Input Multiple-Output (MIMO) PID velocity controller, an extended Kalman filter (EKF) for state estimation, and a maneuvering based dynamic thrust allocation algorithm [28]. The PID controller calculates the desired force,

τ_{cmd} , to achieve the reference velocity ν_{ref} , and the thrust allocation algorithm then determines the necessary thruster forces (see Fig. 8), F_1, F_2, F_3 , and azimuth angles, α_1, α_2 , to apply these commands. Position and velocity predictions are computed using the `robot_localization` package's EKF implementation, as described in [29]. The measurement sources vary based on the setup, as detailed in Section IV.

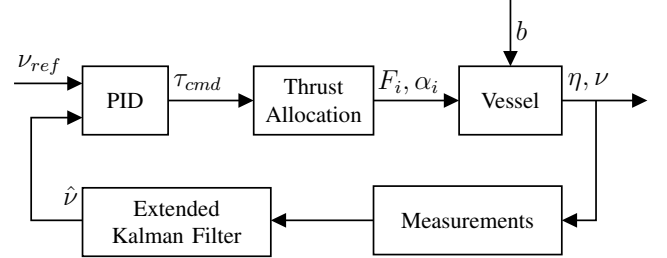


Fig. 6. The low-level velocity control loop of the DP control system.

IV. EXPERIMENTAL SETUP

We test the correct-by-construction hierarchical control architecture in performing autonomous docking maneuvers through simulation and real-world experiments.

A. Simulation

Preliminary testing was conducted in a 3-DOF simulation environment developed for a similar-sized vessel, Cybership (C/S) Enterprise I [30]. C/S Enterprise I is a 1:50 scale tugboat, with dimensions and weight comparable to those of C/S Voyager. The simulation is based on the kinematic and kinetic equations (1) and (2), and uses the Forward Euler method for numerical integration over time. The update equations for the vessel's pose and velocity are given as

$$\eta_{k+1} = \eta_k + \Delta t \cdot \mathbf{R}(\eta_k, \psi) \nu_k, \quad (7a)$$

$$\nu_{k+1} = \nu_k + \Delta t \cdot \mathbf{M}^{-1}(\tau_k - \mathbf{C}(\nu_k) \nu_k - \mathbf{D}(\nu_k) \nu_k), \quad (7b)$$

where Δt represents the time step. Hydrodynamic coefficients for \mathbf{M} , $\mathbf{C}(\nu)$, and $\mathbf{D}(\nu)$ were obtained via system identification in [30]. The simulation environment is implemented using Robot Operating System 2 (ROS 2) and runs in real-time. It models the vessel's surge, sway, and yaw motions by integrating the forces and torques applied by multiple thrusters, utilizing the integrator in (7). The simulator updates the vessel's position (η) and velocity (ν) based on thrust commands received from ROS topics. It then publishes motion data in common ROS interfaces such as odometry and pose.

B. Towing Tank Environment

Experimental trials were conducted in NTNU's Marine Cybernetics Laboratory (MCLab) using a scaled model vessel, the C/S Voyager, in its towing tank. The towing tank has dimensions of $40m \times 6.45m \times 1.5m$, and is equipped with a real-time positioning system, Qualisys, which includes Oqus cameras and the Qualisys Track Manager software. This environment is ideal for testing motion control systems for

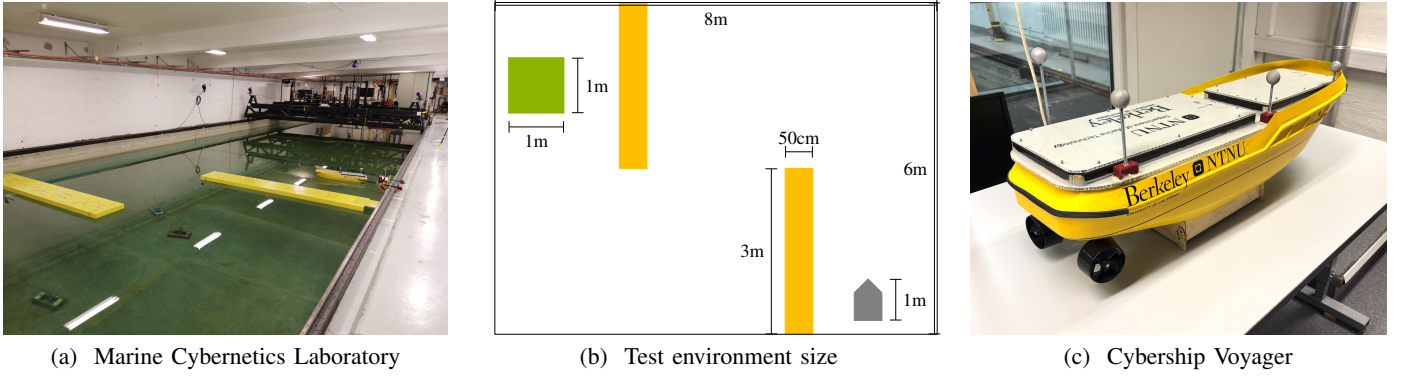


Fig. 7. (a) Marine Cybernetics Laboratory where experiments took place in a towing tank ($40m \times 6.45m \times 1.5m$) with two yellow, two stationary obstacles ($0.5m \times 3m$) attached to the walls and a scaled model vessel (length $1m$). (b) Environment dimensions (c) Model vessel that was used in the experiments

marine vessels, due to its manageable size and advanced instrumentation.

The main test involved two stationary obstacles for the vessel to evade while approaching the target docking position. The testing region for this experiment was a $8m \times 6m \times 1.5m$ portion of the towing tank. In this region, we used 7 motion capturing cameras, ensuring full coverage of the testing area. The two stationary obstacles, each $0.5m \times 3m$, were attached to the walls of the towing tank as depicted in Fig. 7a and 7b.

C. Model Vessel

The C/S Voyager, shown in Fig. 7c, is a 1:32 scale tugboat built at NTNU's MCLab to test advanced navigation and control systems. It is highly maneuverable due to its fast-responding thrusters. The C/S Voyager's azimuth thrusters can reach a maximum force of more than 80N, and it has over 4 hours of endurance. Real-time communication between the vessel's components is made possible by ROS 2, which is installed on a Raspberry Pi 4, the onboard computer. The C/S Voyager has an array of sensing devices, including infrared spheres for accurate position tracking using the Qualisys motion capture system and Inertial Measurement Units (IMUs) for measuring linear accelerations and angular velocity rates. Dimensions of the C/S Voyager are given in Fig. 8.

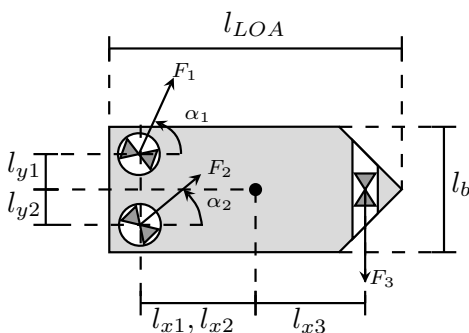


Fig. 8. C/S Voyager dimensions, $l_{y1} = l_{y2} = 7.0cm$, $l_{x1} = l_{x2} = 41.5cm$, $l_{x3} = 37.0cm$, $l_{LOA} = 100.0cm$, and $l_b = 33.0cm$.

D. Optimization Tuning

Since the controller synthesis utilizes a simplified mathematical model of the vessel dynamics, some of the synthesized actions do not correspond to reasonable vessel behavior. For example, it may be safe for the vessel to traverse the docking path backwards; however, it is impractical to exhibit this behavior in the physical world. The matrix W , introduced in Section III-A, ensures that only reasonable actions are chosen.

We designed matrix W to ensure the optimal control action is chosen from the synthesized action set. To determine the value of W , we performed empirical tests and choose the W that provided the smoothest and most realistic vessel behavior. W is chosen conditionally based on the forward velocity component of the proposed control action, $\sigma_{i_{v_x}}$, such that

$$W_i = \begin{cases} \text{diag}(7.5, 3, 1, 1, 1, 2.5) & \sigma_{i_{v_x}} < 0 \\ \text{diag}(1, 6, 1, 1, 1, 2.5) & \text{otherwise.} \end{cases} \quad (8)$$

Given a proposed action with a negative forward velocity, we heavily penalize this backward motion, with weight 7.5, discourage sway motion, with weight 3, and minimize drastic changes in the yaw, with weight 2.5. This ensures that the vessel prioritizes forward motion and limits the usage of the tunnel thruster. Additionally, (8) minimizes rapid rotations of the vessel by maintaining the heading of the vessel, making sure it does not drastically change in a single time step. When a proposed action has a non-negative forward velocity, we only penalize sway motion and changes in the yaw. However, we must increase the sway penalty, with weight 6, as the synthesized controller is more likely to suggest sway commands when we are making forward progress. We similarly discourage vessel rotations and changes in the yaw, with weight 2.5.

V. RESULTS

We executed 2 types of tests on the simulator: experimental validation and dynamic obstacles. First, we mirrored the experimental setup, shown in Fig. 7a, to test the efficacy of our control strategy on both a single obstacle and two obstacles before deploying it on the real vessel. Because we were able to successfully synthesize a control strategy that safely traversed obstacles in simulation, we quickly begin real-world testing.

Additionally, we tested the adaptability of symbolic control in the presence of a dynamic obstacle in the simulation environment. Without adding extra layers of control, we successfully conducted 10 autonomous docking maneuvers while evading a dynamical obstacle. An example of the vessel's behavior in this scenario is shown in Fig. 9. In these tests, the obstacle, sized at $1m \times 1m$, started from the position ($X : 0.5, Y : -2.5$) and moved at a constant velocity of $0.15m/s$ in the positive Y direction. The vessel followed its normal trajectory until the obstacle entered its vicinity at $T = 15s$, at which point the vessel stopped moving until the obstacle had cleared the way before resuming its approach to the docking area, denoted by "End"¹.

Since we did not control the obstacle's path, safety was only ensured against indirect collisions. When the obstacle moved in a path that could lead to a side or head-on collision, avoiding impact was sometimes impossible. This limitation was confirmed through simulations where the obstacle's trajectory directly opposed the vessel's intended docking maneuver. We leave further testing, and refinement of the dynamic obstacle's behavior, as future work.

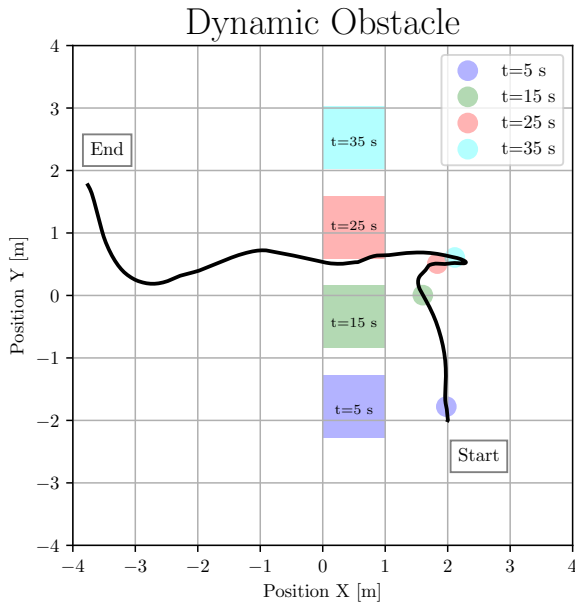


Fig. 9. Example trajectory of a successful autonomous docking in which the vessel evades a square dynamic obstacle. The trajectory of the vessel is shown at various time steps ($t = 5, 15, 25, 35$), along with the position of the dynamic obstacle at that time, to show how the vessel holds a safe position until the obstacle has left the vicinity.

All implementations for the experimental validation were implemented using ROS 2. The necessary subsystems, such as the observers and DP controllers described in Fig. 6, were run on the onboard single board computer. The correct-by-construction synthesis task, as detailed in Section III-A, was performed on a server every two seconds given a state set reflecting this setup as shown in Fig. 1. The resulting velocity commands are guaranteed to maintain vessel safety, given the provable nature of symbolic control.

¹Video of simulated docking maneuvers: <https://www.youtube.com/watch?v=6eLPi4IUyQ8>

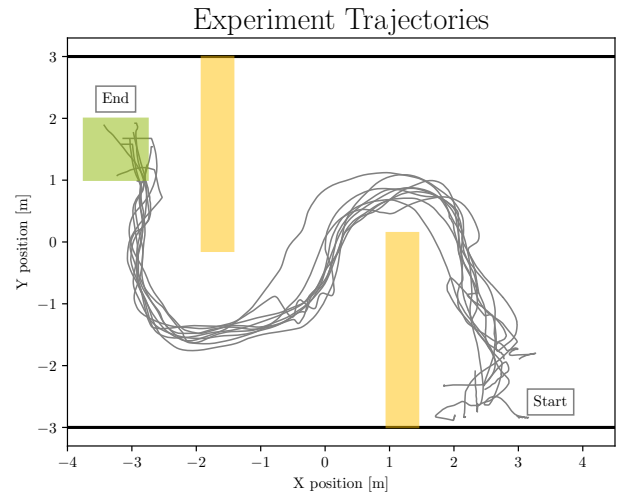


Fig. 10. Trajectories (gray) of 10 successful autonomous docking maneuvers. There was a range of vessel starting positions, the yellow rectangles portray the 3 meter obstacles, and the green box denotes the 1 meter square target.

The trajectories of our successful autonomous docking maneuvers are shown in Fig. 10. The vessel maneuvered generously around the obstacles, allowing extra space to maintain safety and ensure there would be no collisions². On average, the vessel completed this trajectory in 3.41 minutes.

VI. DISCUSSION AND FUTURE WORK

We executed the real-world two-obstacle experiment 25 times, resulting in 10 successful autonomous docking maneuvers. We recognize four categories of experimental issues: communication errors, localization errors, optimization tuning challenges, and synthesis adjustments. During the real-world experiments, network errors led to communication drops lasting between 5 and 20 seconds. Because position measurements were transmitted to the vessel over the network, these interruptions significantly impacted observer accuracy. The synthesis server continued to command new velocities without updated position data, leading to either incomplete runs or erratic vessel behavior due to missing velocity commands. In addition to the network errors, the server was crashing without any error message due to constant polling by the vessel to catch the synthesis state changes. This issue caused experimental failure, discovered only after completion of testing.

Further, we analyzed the ability of the low-level controller to realize the synthesized velocity commands during each successful experiment. To quantify the error between the commanded and realized velocities, we calculated the mean squared error (MSE) of $v_{MSE} = [0.00768m/s, 0.00431m/s, 0.62108deg/s]^T$. How this error in the low-level controller affects the formal guarantees of the proposed approach requires future investigation. We note that this error analysis hints to the robustness of our approach. Even when correctness assumptions on the low-level controller were not met, the accuracy of the low-level controller did not affect the efficacy of the upper-level symbolic control, in many cases.

²Video of successful autonomous docking maneuver in MCLab with model vessel: <https://www.youtube.com/watch?v=q-qohEJciU4>

This system was created with several limitations: it utilizes a simplified vessel model, and it neglects environmental loads, such as wind and waves. In future work, we hope to address these limitations by developing the current vessel model through physics-informed system identification and introducing wave and wind models. Additionally, while we demonstrated the ability of this method to adapt to specific dynamic obstacles without any modifications in simulation, we recognize the need to analyze and test this further in real-world situations. Finally, there are additional applications of this hierarchical symbolic control scheme that could be explored. For example, we will consider an optimization methodology through the development of an energy management system to provide a correct-by-construction control architecture that solves the optimal load sharing problem for vessels.

VII. CONCLUSION

In this paper we have developed a hierarchical symbolic control strategy for the safe autonomous docking of a DP vessel. To validate and verify the proposed design, simulation and experimental trials were presented. The simulation shows the ability of this approach to adapt to new environmental conditions, such as dynamic obstacles, without requiring further levels of control to be developed. Furthermore, the real-world experimental results demonstrate that the vessel can safely traverse a docking path given stationary obstacles.

ACKNOWLEDGMENTS

This paper is supported in part by the NSF Cyber-Physical Systems Frontier project CNS-2111688, NTNU VISTA Centre for Autonomous Robotic Operations Subsea (CAROS), Research Council of Norway (RCN) through SFI AutoShip (RCN project 309230), Guangzhou-HKUST(GZ) Joint Funding Program (Grant No.2023A03J0008), Education Bureau of Guangzhou Municipality, and a grant from the Peder Sather Center for Advanced Study at UC Berkeley. The first author was also supported by a NSF Graduate Research Fellowship. The authors thank Emil Bratlie, Robert Opland, Terje Rosten, Vebjørn Steinsholt, Gabriel Bjørgan Vikan, and Anne Elise Havmo for facilitating experimentation in the MCLab.

REFERENCES

- [1] K. Wróbel, J. Montewka, and P. Kujala, "Towards the assessment of potential impact of unmanned vessels on maritime transportation safety," *Reliability Engineering & System Safety*, vol. 165, pp. 155–169, 2017.
- [2] A. J. Sørensen, "A survey of dynamic positioning control systems," *Annual reviews in control*, vol. 35, no. 1, pp. 123–136, 2011.
- [3] S. J. Simonlexau, M. Breivik, and A. M. Lekkas, "Automated docking for marine surface vessels—a survey," *IEEE Access*, vol. 11, pp. 132 324–132 367, 2023.
- [4] C. Baier and J.-P. Katoen, *Principles of model checking*. MIT press, 2008.
- [5] X. Yin, B. Gao, and X. Yu, "Formal synthesis of controllers for safety-critical autonomous systems: Developments and challenges," *Annual Reviews in Control*, vol. 57, p. 100940, 2024.
- [6] P. Tabuada, *Verification and control of hybrid systems: a symbolic approach*. Springer Science & Business Media, 2009.
- [7] G. Reissig, A. Weber, and M. Rungger, "Feedback refinement relations for the synthesis of symbolic controllers," *IEEE Transactions on Automatic Control*, vol. 62, no. 4, pp. 1781–1796, 2016.
- [8] B. Zhong, A. Lavaei, M. Zamani, and M. Caccamo, "Automata-based controller synthesis for stochastic systems: A game framework via approximate probabilistic relations," *Automatica*, vol. 147, p. 110696, 2023.
- [9] M. Rungger and M. Zamani, "SCOTS: A tool for the synthesis of symbolic controllers," in *Proceedings of the 19th International Conference on Hybrid Systems: Computation and Control*, 2016, pp. 99–104.
- [10] M. Khaled and M. Zamani, "pFaces: An acceleration ecosystem for symbolic control," in *Proceedings of the 22nd International Conference on Hybrid Systems: Computation and Control*, 2019, pp. 252–257.
- [11] W. Cai, M. Zhang, Q. Yang, C. Wang, and J. Shi, "Long-range UWB positioning based automatic docking trajectory design for unmanned surface vehicle," *IEEE Transactions on Instrumentation and Measurement*, 2023.
- [12] S. Yuan, Z. Liu, Y. Sun, Z. Wang, and L. Zheng, "An event-triggered trajectory planning and tracking scheme for automatic berthing of unmanned surface vessel," *Ocean Engineering*, vol. 273, p. 113964, 2023.
- [13] K. Bergman, O. Ljungqvist, J. Linder, and D. Axehill, "An optimization-based motion planner for autonomous maneuvering of marine vessels in complex environments," in *IEEE Conference on Decision and Control (CDC)*, 2020, pp. 5283–5290.
- [14] Ø. Volden, A. Stahl, and T. I. Fossen, "Development and experimental validation of visual-inertial navigation for auto-docking of unmanned surface vehicles," *IEEE Access*, 2023.
- [15] S. Baek and J. Woo, "Model reference adaptive control-based autonomous berthing of an unmanned surface vehicle under environmental disturbance," *Machines*, vol. 10, no. 4, p. 244, 2022.
- [16] S. Kockum, "Autonomous docking of an unmanned surface vehicle using model predictive control," Ph.D. dissertation, Master's thesis. Lund University, 2022.
- [17] S. Wang, Z. Sun, Q. Yuan, Z. Sun, Z. Wu, and T.-H. Hsieh, "Autonomous piloting and berthing based on long short time memory neural networks and nonlinear model predictive control algorithm," *Ocean Engineering*, vol. 264, p. 112269, 2022.
- [18] DNV GL. (2018) Class guidelines for autonomous and remotely operated ships. DNVGL-CG-0264, Edition September 2018. [Online]. Available: <https://www.dnv.com/maritime/autonomous-remotely-operated-ships/class-guideline/>
- [19] P.-J. Meyer, H. Yin, A. H. Brodtkorb, M. Arcak, and A. J. Sørensen, "Continuous and discrete abstractions for planning, applied to ship docking," *IFAC-PapersOnLine*, vol. 53, no. 2, pp. 1831–1836, 2020.
- [20] B. Zhong, H. Cao, M. Zamani, and M. Caccamo, "Towards safe AI: Sandboxing dnns-based controllers in stochastic games," in *Proceedings of the AAAI Conference on Artificial Intelligence*, vol. 37, no. 12, 2023, pp. 15 340–15 349.
- [21] M. K. M. Mahmoud, "Efficient implementation of symbolic controllers for cyber-physical systems," Ph.D. dissertation, Technichal University of Munich, 2021.
- [22] T. I. Fossen, *Handbook of marine craft hydrodynamics and motion control*. John Wiley & Sons, 2011.
- [23] M. Zamani, G. Pola, M. Mazo, and P. Tabuada, "Symbolic models for nonlinear control systems without stability assumptions," *IEEE Transactions on Automatic Control*, vol. 57, no. 7, pp. 1804–1809, 2012.
- [24] P. Tabuada, *Verification and Control of Hybrid Systems: A Symbolic Approach*, 1st ed. Springer Publishing Company, Incorporated, 2009.
- [25] M. Khaled, K. Zhang, and M. Zamani, "A framework for output-feedback symbolic control," *IEEE Transactions on Automatic Control*, vol. 68, no. 9, pp. 5600–5607, 2023.
- [26] C. Dawson, A. Jasour, A. Hofmann, and B. Williams, "Provably safe trajectory optimization in the presence of uncertain convex obstacles," in *2020 IEEE/RSJ International Conference on Intelligent Robots and Systems (IROS)*. IEEE, 2020, pp. 6237–6244.
- [27] B. Axelrod, L. P. Kaelbling, and T. Lozano-Pérez, "Provably safe robot navigation with obstacle uncertainty," *The International Journal of Robotics Research*, vol. 37, no. 13-14, pp. 1760–1774, 2018.
- [28] E. C. Gezer and R. Skjetne, "Maneuvering-based dynamic thrust allocation for fully-actuated vessels," *IFAC-PapersOnLine*, vol. 58, no. 20, pp. 374–379, 2024.
- [29] T. Moore and D. Stouch, "A generalized extended kalman filter implementation for the robot operating system," in *Proceedings of the 13th International Conference on Intelligent Autonomous Systems (IAS-13)*. Springer, July 2014.
- [30] H. N. Skåtun, "Development of a DP system for CS Enterprise I with Voith Schneider thrusters," Master's thesis, Norwegian University of Science and Technology, 2011.